PAPER

Effective n-type F-doped MoSe$_2$ monolayers

Xu Zhao, [iD] *[a] Xiaonan Zhang,[a] Tianxing Wang,[a] Shuyi Wei*[a] and Lin Yang[b]

Using a first-principles method, based on the Vienna Ab-initio Simulation Package (VASP), we have studied the electronic structure, formation energy and transition level of a MoSe$_2$ monolayer doped with V and VII atoms. The numerical results show that the dopant atoms can induce magnetism, except for in the case of the As-doped system. Specifically, N- and F-doped systems exhibit magnetic nanomaterial properties, P- and As-doped systems display metallic features, and in the cases of Cl-, Br- and I-doped systems, the systems exhibit half-metallic ferromagnetism (HMF). The formation energy calculations indicate that this can be more effective for achieving n-type and p-type doped MoSe$_2$ under Mo-rich experimental conditions. However, for the systems doped with group V atoms, the transition level decreases with increasing atomic radius, but that of those doped with VII atoms increases with increasing atomic radius. By comparing the results, we find that the transition level is only 31 meV in F-doped MoSe$_2$ monolayers, which indicates that F impurities can offer effective n-type carriers in MoSe$_2$ monolayers.

1. Introduction

In recent years, two dimensional materials have received great attention, mainly due to their excellent performance, which can meet the flexibility, adaptability and multifunctional requirements of the fields of optoelectronics and nanoelectronics.[1–3] In particular, transition metal dichalcogenides (TMDs), expressed as MX$_2$, with semiconducting properties could replace graphene as the best material to construct nanomaterial devices. Although they have structure properties that are similar to that of graphene, TMDs such as WS$_2$, WSe$_2$, MoS$_2$, and MoSe$_2$ have band gaps of 1–2 eV,[4,5] making them promising for low-dimensional engineering devices. At present, they can be applied to field effect transistors,[6,7] optoelectronic devices,[8] transducers,[9] and for hydrogen storage.[10,11] Perfect MoSe$_2$, MoTe$_2$ and WS$_2$ exhibit the quantum confinement effect, which induces indirect-direct-gap crossover characteristics.[12] In particular, some experimental studies have pointed out that when the two-dimensional materials are only several atomic layers thick, their structures are similar to that of graphene with a layered hexagonal structure, and the band gaps transform from indirect to direct as the thickness decreases.[13] Excitingly, their electrical and magnetic properties can be controlled *via* doping with different atoms.[14,15] It is well known that impurity states play an important role in semiconducting optoelectronic devices in controlling the carrier concentration and conductivity of the materials.[16,17] Moreover, previous research has carried out calculations on the electronic structure of a MoS$_2$ monolayer, aiming to determine whether the MoS$_2$ monolayer could be used in device manufacturing with n- and p-doping, and they concluded that n- and p-type semiconductor devices can be prepared under the appropriate doping conditions.[18] Furthermore, our groups have confirmed that some semiconductors could be induced to have half-metallic ferromagnetism (HMF) by means of introducing nonmagnetic atoms in the MoS$_2$ monolayer.[19] It is generally known that half-metal materials have the characteristics of both metals and insulators, and studies have found that the spin polarization rate of a half-metal can reach 100% at a Curie temperature that is above room temperature.[20,21] Therefore, there is no doubt that they can be used as spin injection sources for semiconductor devices.[22]

In order to realize the electronic and optoelectronic properties of MoSe$_2$ more widely used, an efficient and controllable n- and p-type doping technology is indispensable.[23–25] In spite of the many experimental and related theoretical studies that have been done, understanding the MoSe$_2$ monolayer conductive mechanism is still worthy of further research and development. Hence, in this work, we research the characteristics of n-type and p-doped MoSe$_2$ monolayers, using group V and VII atoms as substitutes for the Se atoms in the MoSe$_2$ monolayers, using first principles methods. The results of our calculations show that this can be more effective for achieving n-type and p-type doped semiconductors under Mo-rich experimental conditions. Moreover, the transition level of the F-doped MoSe$_2$ monolayer is only 31 meV, thus we consider F impurities to be the best choice for achieving n-type conductivity. These results will be meaningful to understand the characteristics of n-type and p-doped MoSe$_2$ monolayers.

The paper structure is as follows. In Section 2, we give the theoretical basis of the paper and introduce the related calculation methods. In Section 3, we investigate the electronic

[a]College of Physics and Materials Science, Henan Normal University, Xinxiang, Henan 453007, China. E-mail: zhaoxu@htu.cn

[b]School of Chemistry and Chemical Engineering, Henan Normal University, Xinxiang, Henan 453007, China

structures, formation energies, and transition energy levels of the MoSe$_2$ monolayers using first principles calculations, and Section 4 is a summary of this work.

2.   Calculation models and methods

All of our calculations are performed with first principles methods based on density functional theory (DFT), and we use the Projected Augmented Wave (PAW) method to describe the interaction between the valence electrons and the ions.[26,27] In addition, we also adopt the PBE generalized gradient approximation functional in the form of the Generalized Gradient Approximation (GGA) to describe the electronic exchange correlation potential.[28–30] The single electron state was expanded by the plane wave basis set, and the energy cut off that we selected for the plane-wave expansion of the wave functions is 500 eV. The valence electron configurations were Se(4s^{2}p^4), Mo(4d^{5}5s^1), N(2s^{2}p^3), P(3s^{2}p^3), As(4s^{2}p^3), F(2s^{2}p^5), Cl(3s^{2}p^5), Br(4s^{2}p^5) and I(5s^{2}p^5), and the special k-point sampling of the Monkhorst–Pack scheme was applied for the Brillouin-zone integrations. For the Brillouin-zone sampling, a $9 \times 9 \times 1$ Monkhorst–Pack k mesh was selected for the $4 \times 4 \times 1$ unit cells. When the doping atom is at a Se site, the doping concentration is 3.12% for each doping system,[31] and the interaction between the dopant atoms in the neighboring cells is negligible, which indicates that the doping concentration that we used (3.12%) may be appropriate for studying the electronic and magnetic properties of the group V and VII atom doped MoSe$_2$ monolayers. The vacuum layer thickness we set was 15 Å to reduce the artificial interactions between the two surfaces. In order to maintain the accuracy, the total convergence of the system was taken as 10^{-5} eV. The structure optimization was carried out until all of the atomic forces on each ion were less than 0.01 eV Å^{-1}, and the lattice constant of the optimized system always reached the minimum value. Beyond the aim of comparison the electronic structures with the results from the GGA method, we have taken the effects of the on-site Coulomb repulsion of Mo-4d electrons into account by calculating the exchange–correlation energy using the GGA + U method,[32] where the U parameter is chosen to be 3.0 eV for the Mo-4d orbital, which was used in previous theoretical studies.[33,34]

3.   Results and discussion

In brief, MoSe$_2$ is structurally similar to graphene, as it consists of covalently bonded Se–Mo–Se 2D hexagonal planes, as shown in Fig. 1. Each atomic layer relies on weak van der Waals forces to form massive crystals. In this system, the electrons are limited to moving in a two dimensional direction, and the M–X covalent bond is formed by the hybridization of p–d orbitals.

3.1   Formation energy and transition level of impurities in MoSe$_2$ monolayers

As we all know, the formation energy is the vital parameter to confirm a system's stability. To get a more stable system,
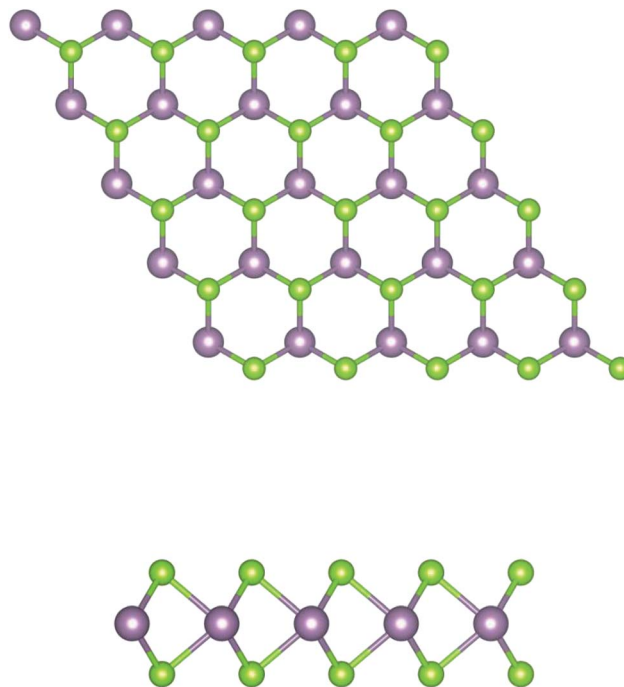

Fig. 1 Schematic structure of a MoSe$_2$ monolayer. The top and side views of the layered forms are shown. The purple and green balls represent the Mo and Se atoms, respectively.

group V and VII atom doped MoSe$_2$ monolayers were calculated in this work separately. As shown in Table 1, we list the values of $d_{\text{Mo–X}}$ (X denotes the group V and VII atoms), M_{Mo}, M_{X}, M_{tot}, E_{doped} and E_{form} (under different experimental conditions). By comparison, it is shown that the bond length $d_{\text{Mo–X}}$ and the formation energy also increase with the increase of the radii of the group V or VII atoms. The total energy of the N-doped MoSe$_2$ case was the lowest, which indicates that the N-doped MoSe$_2$ monolayer is much more stable than the other considered impurity cases. To examine availability of n- and p-type doping in MoSe$_2$, the formation energy could be calculated using the following formula:[35]

$$E_{\text{form}}{}^q = E_{(\text{doped})}{}^q - E_{(\text{pure})} - \sum n_i \mu_i + q[E_F + E_v + \Delta V] \quad (1)$$

where $E_{\text{form}}{}^q$ and $E_{(\text{pure})}$ are the total energies of the charged and neutral systems, respectively, n_i (i = Mo, Se and X) represents the number of atoms that has been incorporated ($n_i > 0$) or replaced ($n_i < 0$), and μ_i is used to express the chemical potential in the case of lowest energy E_i. E_F is the Fermi level referenced to the energy position (E_v) of the valence band maximum (VBM) for pure MoSe$_2$, and varies from 0 to E_g. In addition, ΔV is used as the correction term to align the reference potential in the doped supercell with that in pure MoSe$_2$ with the same size supercells.[36] Furthermore, q indicates the number of charges introduced to the calculated system. The transition energy levels of the acceptor ($q < 0$) and the donor ($q > 0$) relative to the conduction band minimum (CBM) can be found using the following equation:[37]

$$\varepsilon_D\left(q/q'\right) = \frac{E_{\text{form}}{}^q - E_{\text{form}}{}^{q'}}{q' - q} \quad (2)$$

Table 1 The calculated d_{Mo-X} (Mo–X bond length), magnetic moment M_{Mo}, M_X, M_{tot}, E_{doped}, transition level $\varepsilon_D(q/q')$ and E_{form} (under different experimental conditions)

System	d_{Mo-X} (Å)	M_{Mo} (μ_B)	M_X (μ_B)	M_{tot} (μ_B)	E_{doped} (eV)	$\varepsilon_D(q/q')$ (eV)	E_{form} Mo-rich	Se-rich
N	2.004	0.024	0.197	0.790	−322.336	0.207	0.481	1.518
P	2.411	0.069	0.068	0.553	−319.449	0.155	1.135	2.173
As	2.575	0.0	0.0	0.0	−318.597	0.150	4.021	5.059
F	2.284	0.231	0.056	0.885	−317.873	0.031	−1.306	−0.268
Cl	2.515	0.253	0.044	0.872	−316.285	0.103	0.217	1.255
Br	2.650	0.260	0.055	0.892	−315.621	0.125	1.025	2.063
I	2.821	0.253	0.062	0.867	−314.975	0.199	1.563	2.601

where E_{form}^q and $E_{form}^{q'}$ are the formation energies of X-doped MoSe$_2$ with charge states. It is worth noting that the formation of the doped system is closely related to the experimental conditions of the system. Under Mo-rich conditions, the chemical potential of the Mo atoms can be obtained by calculating the total energy of the bulk Mo, and the chemical potential of the Se atoms can be obtained by the following equation:

$$2\mu_{Se} + \mu_{Mo} = \mu_{MoSe_2} \quad (3)$$

From the above calculations, we see that the formation energy is lower under Mo-rich conditions than under Se-rich conditions, and the N-doped MoSe$_2$ monolayer is much more stable than the other considered impurity cases. To have a better understanding, Fig. 2 is given to describe the formation energies and transition levels of group V and VII atom doped MoSe$_2$, and we present the formation energies as a function of the Fermi level referenced to the VBM in the MoSe$_2$ monolayers. For p-type doping cases, one can see that the formation energy curves move towards the VBM with increasing atomic number of the dopant, and this indicates that, along with the atomic number increasing, the transition level between the different charge states (0/−1) decreases. The numerical results show that the calculated transition levels are 207 meV, 155 meV, and 150 meV above the VBM for the N-, P-, and As-doped MoSe$_2$, respectively. From the transition level data, it can be concluded that group V impurities are shallow acceptor dopants in MoSe$_2$ monolayers. But for the case of the n-type doped system, the charge state (+1/0) transition levels are 31 meV, 103 meV, 125 meV, and 199 meV below the CBM, for the F-, Cl-, Br- and I-doped MoSe$_2$, respectively, which indicates the halogen impurities are shallow donor dopants in MoSe$_2$ monolayers. From these data, we can see that when the atomic number increases, the transition level of the charged system also increases. This trend is the opposite of the former, which may be attributed to the stronger electronegativity of halogen atoms compared to group V atoms. Therefore, we predicted that n-type conductivity may be engineered in the group VII atom doped MoSe$_2$ systems *via* halogen atom doping. Furthermore, combining the above transition level data, the transition level of the F impurities is only 31 meV, thus we consider that F impurities can offer effective n-type carriers in MoSe$_2$ monolayers.

3.2 Electronic structures of group V and VII atoms doped in MoSe$_2$ monolayers

Fig. 3(a) shows the band structures for the pristine and X-doped MoSe$_2$ monolayers using the GGA method. For the pristine MoSe$_2$ monolayer, the direct band gap at high symmetry is about 1.51 eV, which supplies a reliable basis to confirm that the pristine monolayer is a semiconductor. Indeed, it is consistent with previous theoretical and experimental results.[38]
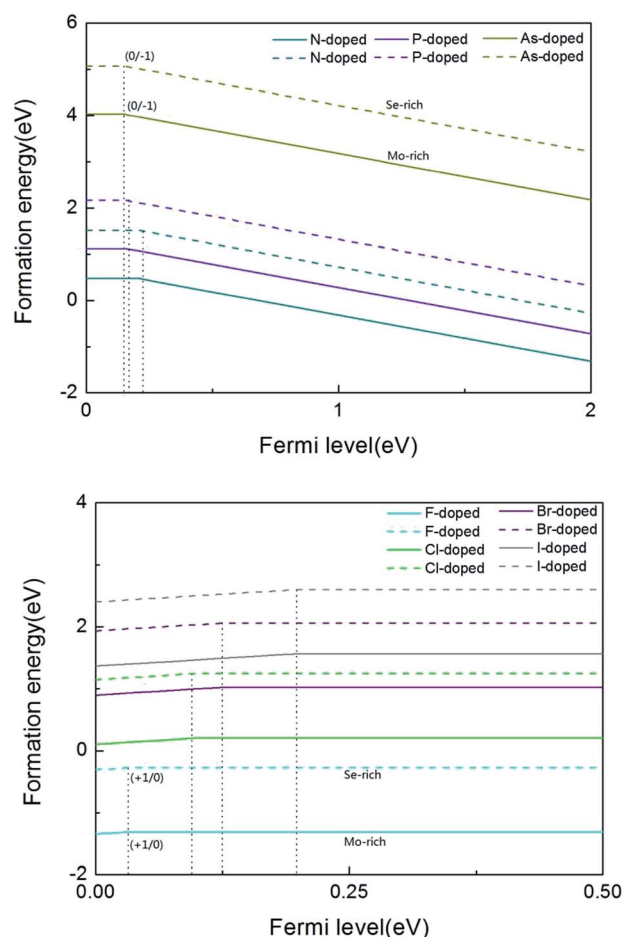

Fig. 2 The formation energy as a function of Fermi level from the VBM to CBM for group V and VII dopant atoms. In both of the figures, the solid line represents the Mo-rich cases and the broken line represents the Se-rich cases.

Due to the introduction of dopant atoms, an impurity state appeared in the band structures. In addition, the impurity states are close to the valance band in the N-, P-, and As-doped systems, and this signifies that the systems are p-type doped. But for the F-, Cl-, Br- and I-doped systems, the impurity states are close to the conduction band, which indicates n-type doping. From Fig. 3(a), we find that the pure $MoSe_2$ monolayer is an intrinsic semiconductor without magnetism. However, the group V and VII atoms can induce magnetism, in addition to the As-doped system. This is due to the fact that as the atomic number increases, the bond length increases, but the bond energy decreases. The results of our calculations show that the formation energy of the As-doped system is larger than that of the N- and P-doped systems and the interaction with the host atoms is weaker. The electronegativity of As atoms is smallest compared to that of the other dopant atoms in group V and VII. More specifically, N- and F-doped systems exhibit magnetic nanomaterial properties, and the P- and As-doped systems display metallic features. Cl-, Br-, and I-doped systems exhibit half-metal features. The half-metallic (HM) gap is a valuable parameter for ensuring whether half-metallic ferromagnetic materials could be ideal electron spin injection sources for semiconductors, and is defined as the minimum of E_c and E_v, where E_c is the energy of the bottom of the minority-spin conduction band and E_v is the absolute energy value of the top of the minority-spin valence band, and both of these values are quoted with respect to the Fermi level.[16,19] According to this rule, the HM gaps that we calculated for the Cl-, Br-, and I-doped systems are about 0.035 eV, 0.049 eV, and 0.071 eV, respectively. HM material with a spin polarization that is close to 100% near the Fermi level ensures the passage of the preferred spin at a high degree, and thus the Cl-, Br-, and I-doped systems may be feasible for spin filter device applications.[20,39]

In addition, the previous theoretical studies on 2D Mo systems usually neglected the GGA + U method[31,40] because Mo is not a strongly correlated system,[41] and so a relatively small value for the on-site Coulomb interaction is sufficient for the calculated systems.[42] To get more accurate results, we have recalculated it using the GGA + U method with $U = 3.0$ eV. The magnetic moments we calculated for the group V and VII atom doped $MoSe_2$ systems are 0.856 μ_B, 0.623 μ_B, 0.002 μ_B, 1.024 μ_B, 0.962 μ_B, 0.982 μ_B, and 0.911 μ_B, respectively, which are similar to the results achieved using the GGA method in Table 1. We also chose the N- and F-doped systems as representative cases to plot the band structure graph in Fig. 3(b), and found that it did not affect our conclusions that were drawn from using the GGA method. Thus, we hold the above view that the group V and VII atom doped systems are not sensitive to the value of U through our calculations using the GGA + U approach.

Furthermore, to more fully explain the electronic structures of $MoSe_2$ monolayers, the total density of states (TDOS) and partial total density of states (PDOS) of the doped systems are shown in Fig. 4. As shown in the graphs, some impurity states appear in the gap, thus leading to the DOS of spin-up and spin-down systems to be asymmetric near the Fermi energy compared to that of the perfect $MoSe_2$ monolayer. It also reveals
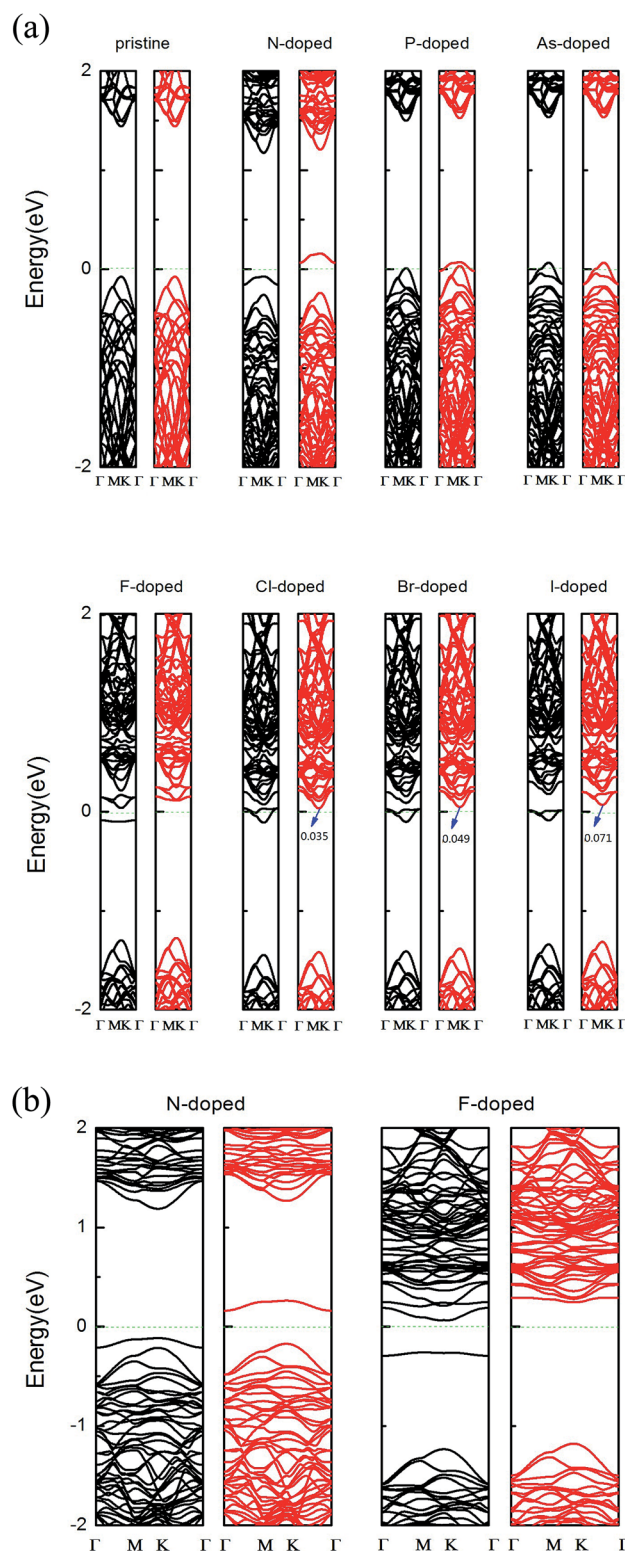

Fig. 3 (a) Band structures of pristine and one X-doped $MoSe_2$ monolayer using the GGA method. The black lines and red lines represent the spin-up and spin-down components, respectively, where the Fermi level is indicated by the dotted line. (b) The band structures of typical N- and F-doped $4 \times 4 \times 1$ $MoSe_2$ monolayers using the GGA + U method.
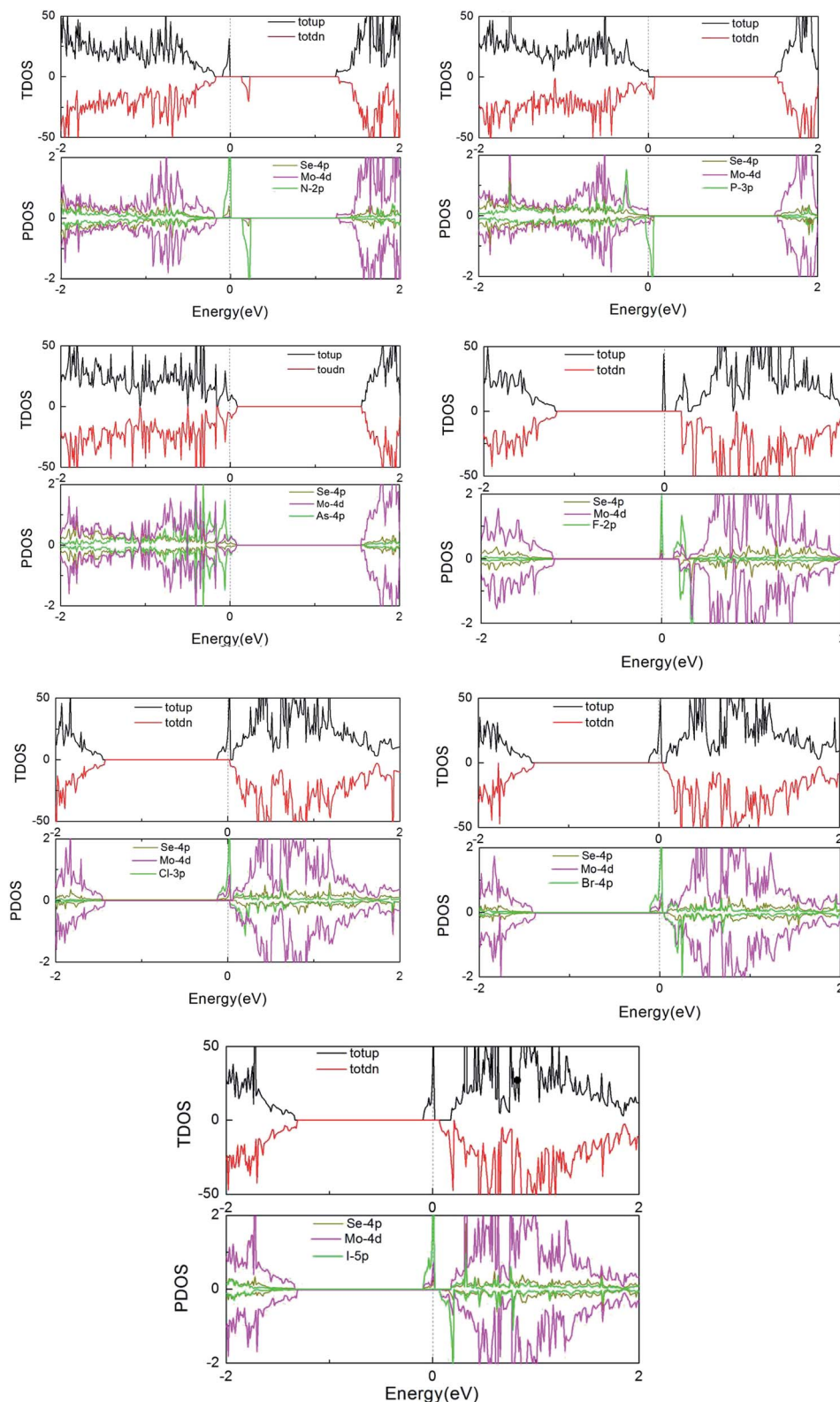
Fig. 4 TDOS and PDOS of the X dopants and their neighboring Mo and Se atoms in the X-doped $4 \times 4 \times 1$ $MoSe_2$ monolayer.

that the local moment is mainly contributed to by the p orbital of the Se atoms and the d orbital of the Mo atoms. The hybridization between the Mo-4d and Se-4p states is associated with the weak covalency between the Mo and Se atoms. For pristine and As-doped systems, the spin-up and spin-down TDOS are symmetric, which indicates that the pure system

presents a non-magnetic ground state,[16] which agrees exactly with the calculated total magnetic moment 0 μ_B for the systems (see Table 1). But for the other doped systems, the spin-up and spin-down TDOS are asymmetric, which indicates that the systems present a magnetic ground state. These conclusions are also consistent with the results in Table 1. Moreover, the impurity states of the doped systems are mostly derived from the X-p orbitals, with a small part from the Mo-4d and Se-4p orbitals near the Fermi level. An asymmetrical distribution of the DOS can be seen between the majority spin and minority spin states, which produces magnetism in the X doped systems (except for the As-doped system), and the magnetic property mainly originates from the p–d hybridization between the p orbitals of the doped X atoms and the d orbitals of the neighboring three Mo atoms.

4. Conclusions

In summary, we investigated the electronic structure, formation energy, and transition energy level of $MoSe_2$ based on density functional theory. The calculated results show that group V and VII atom doping can induce magnetism, except for in the As-doped system. The impurity bands of the doped systems are mostly derived from the Mo-4d orbitals near the Fermi level. N- and F-doped $MoSe_2$ monolayers exhibit magnetic nanomaterial features. P- and As-doped $MoSe_2$ show magnetic metallic features. The Cl-, Br-, and I-doped systems exhibit half-metallic ferromagnetism (HMF), and their half-metallic gap is about 0.035 eV, 0.049 eV, and 0.071 eV, respectively. The group V atom doped systems have p-type doping and the group VII atom doped systems can be defined as having n-type doping. The formation energy shows that the system is more stable under Mo-rich experimental conditions. In particular, for group V atom doped $MoSe_2$, the transition level decreases with the increase of the atomic radius, but for the group VII atom doped systems, it is the opposite. By comparison, the transition energy level of F impurities is only 31 meV, thus we consider that F impurities can offer effective n-type carriers in $MoSe_2$ monolayers. These results may be interesting for shedding light on further experimental investigations of n-type doping in $MoSe_2$ monolayer systems.

Acknowledgements

References

1 Q. H. Wang, K. Kalantar-Zadeh, A. Kis, J. N. Coleman and M. S. Strano, *Nat. Nanotechnol.*, 2012, **7**, 699–712.

2 M. Xu, T. Liang, M. Shi and H. Chen, *Chem. Rev.*, 2013, **113**, 3766–3798.

3 F. H. L. Koppens, T. Mueller, P. Avouris, A. C. Ferrari, M. S. Vitiello and M. Polini, *Nat. Nanotechnol.*, 2014, **9**, 780–793.

4 A. Kumar and P. K. Ahluwalia, *Eur. Phys. J. B*, 2012, **85**, 186.

5 P. R. Villeneuve and M. Piche, *Phys. Rev. B: Condens. Matter Mater. Phys.*, 1992, **46**, 4969.

6 F. Garnier, R. Hajlaoui, A. Yassar and P. Srivastava, *Science*, 1994, **265**, 1684–1687.

7 A. Tsumura, H. Koezuka and T. Ando, *Appl. Phys. Lett.*, 1986, **49**, 1210–1212.

8 Y. Li, F. Qian, J. Xiang and C. M. Lieber, *Mater. Today*, 2006, **9**, 18–27.

9 T. T. Wu, L. C. Wu and Z. G. Huang, *J. Appl. Phys.*, 2005, **97**, 094916.

10 L. Schlapbach and A. Züttel, *Nature*, 2001, **414**, 353–358.

11 A. Dillon, K. M. Jones, T. A. Bekkedahl and C. H. Kiang, *Nature*, 1997, **386**, 377.

12 R. Mishra, W. Zhou, S. J. Pennycook, S. T. Pantelides and J. C. Idrobo, *Phys. Rev. B: Condens. Matter Mater. Phys.*, 2013, **88**, 144409.

13 J. N. Coleman, M. Lotya, A. O'Neill, S. D. Bergin, P. J. King, U. Khan and I. V. Shvets, *Science*, 2011, **331**, 568–571.

14 X. Zhao, C. X. Xia, T. X. Wang, X. Q. Dai and L. Yang, *J. Alloys Compd.*, 2016, **689**, 302–306.

15 X. Zhao, T. X. Wang, G. X. Wang, X. Q. Dai, C. X. Xia and L. Yang, *Appl. Surf. Sci.*, 2016, **383**, 151–158.

16 Y. Ma, Y. Dai, M. Guo, C. Niu, Y. Zhu and B. Huang, *ACS Nano*, 2012, **6**, 1695–1701.

17 Y. C. Cheng, Z. Y. Zhu, W. B. Mi, Z. B. Guo and U. Schwingenschlögl, *Phys. Rev. B: Condens. Matter Mater. Phys.*, 2013, **87**, 100401.

18 K. Dolui, I. Rungger, C. D. Pemmaraju and S. Sanvito, *Phys. Rev. B: Condens. Matter Mater. Phys.*, 2013, **88**, 075420.

19 X. Zhao, P. Chen, C. X. Xia, T. X. Wang and X. Q. Dai, *RSC Adv.*, 2016, **6**, 16772–16778.

20 Y. H. Zhao, G. P. Zhao, Y. Liu and B. G. Liu, *Phys. Rev. B: Condens. Matter Mater. Phys.*, 2009, **80**, 224417.

21 Y. Li, Z. Zhou, P. Shen and Z. Chen, *ACS Nano*, 2009, **3**, 1952–1958.

22 R. A. de Groot, F. M. Mueller, P. G. van Engen and K. H. J. Buschow, *Phys. Rev. Lett.*, 1983, **50**, 2024.

23 H. Li, X. Duan, X. Wu, X. Zhuang, H. Zhou, Q. Zhang and L. Ma, *J. Am. Chem. Soc.*, 2014, **136**, 3756–3759.

24 H. Ohno, A. Shen, F. Matsukura, A. Oiwa, A. Endo, S. Katsumoto and Y. Iye, *Appl. Phys. Lett.*, 1996, **69**, 363.

25 X. Zhao, C. X. Xia, T. X. Wang and X. Q. Dai, *J. Alloys Compd.*, 2016, **654**, 574–579.

26 J. Hafner, *J. Comput. Chem.*, 2008, **29**, 2044–2078.

27 W. Chen, E. J. Santos, W. Zhu, E. Kaxiras and Z. Zhang, *Nano Lett.*, 2013, **13**, 509–514.

28 J. P. Perdew, K. Burke and M. Ernzerhof, *Phys. Rev. Lett.*, 1996, **77**, 3865.

29 P. E. Blöchl, *Phys. Rev. B: Condens. Matter Mater. Phys.*, 1994, **50**, 17953.

30 G. Kresse and D. Joubert, *Phys. Rev. B: Condens. Matter Mater. Phys.*, 1999, **59**, 1758.

31 Y. Ma, Y. Dai, M. Guo, C. Niu, J. Lu and B. Huang, *Phys. Chem. Chem. Phys.*, 2011, **13**, 15546–15553.

32 S. L. Dudarev, G. A. Botton, S. Y. Savrasov, C. J. Humphreys and A. P. Sutton, *Phys. Rev. B: Condens. Matter Mater. Phys.*, 1998, **57**, 1505.

33 X. Du, Q. Li, H. Su and J. Yang, *Phys. Rev. B: Condens. Matter Mater. Phys.*, 2006, **74**, 233201.

34 P. Liu, Z. Z. Qin, Y. L. Yue and X. Zuo, *Chin. Phys. B*, 2017, **26**, 027103.

35 C. G. Van de Walle and J. Neugebauer, *J. Appl. Phys.*, 2004, **95**, 3851–3879.

36 C. X. Xia, X. Zhao, Y. T. Peng, H. Zhang, S. Y. Wei and Y. Jia, *Superlattices Microstruct.*, 2015, **85**, 664–671.

37 S. H. Wei, *Comput. Mater. Sci.*, 2004, **30**, 337–348.

38 S. Tongay, J. Zhou, C. Ataca, K. Lo, T. S. Matthews, J. Li and J. Wu, *Nano Lett.*, 2012, **12**, 5576–5580.

39 R. A. De Groot, F. M. Mueller, P. G. Van Engen and K. H. J. Buschow, *Phys. Rev. Lett.*, 1983, **50**, 2024.

40 J. He, K. Wu, R. Sa, Q. Li and Y. Wei, *Appl. Phys. Lett.*, 2010, **96**, 082504.

41 A. Splendiani, L. Sun, Y. Zhang, T. Li, J. Kim, C. Chim and F. Wang, *Nano Lett.*, 2010, **10**, 1271–1275.

42 S. Lebegue and O. Eriksson, *Phys. Rev. B: Condens. Matter Mater. Phys.*, 2009, **79**, 115409.